CHEMICAL ENGINEERING TRANSACTIONS
VOL. 60, 2022
A publication of AIDIC
The Italian Association of Chemical Engineering
Online at www.cetjournal.it
Guest Editors: Petar S. Varbanov, Yee Van Fan, Jiří J. Klemeš, Sandro Nižetić

ISBN 978-88-95608-93-8; **ISSN** 2283-9216
DOI: 10.3303/CET2294031

Numerical Study on Shell-and-Tube Moving Packed Bed Heat Exchanger: Effect of Tube Arrangement on the Particle Side

Xing Tian, Haonan Jia, Jiayue Zhang, Zhigang Guo, Jian Yang*, Qiuwang Wang

MOE Key Laboratory of Thermo-Fluid Science and Engineering, School of Energy and Power Engineering, Xi'an Jiaotong University, Xi'an 710049, China
yangjian81@mail.xjtu.edu.cn

Moving packed bed heat exchanger has been key equipment in the waste energy recovery and concentrated solar power. However, the effect of tube arrangement still deserve investigation to optimize heat transfer. In the present paper, the flow and heat transfer of gravity-driven particles flowing around the tube bank are numerically studied by the discrete element method. It was found that the stagnation zone of the staggered tubes is less than 45° and the cavity zone is in the range of 160° - 180°. The stagnation zone of the aligned tubes is in the range of 0° - 65° and 125° - 180°, and there is no cavity zone below the aligned tubes. The heat transfer performance of the staggered tubes is better than that of the aligned tubes. The best heat transfer region of the staggered tubes is at the top of the tube, and that of the aligned tubes is at the side of the tube. The bottom of the tube has the worst heat transfer in both the staggered and aligned tubes. It is necessary to improve the performance of the staggered tubes by optimizing the particle flow in the range 0° - 45° and 160° - 180°. Reducing the vertical tube spacing may be an effective option for the aligned tubes.

1. Introduction

With the increasing trend of global warming, energy transformation and the development of clean and energy-saving technologies have attracted much attention. The development of waste energy recovery and concentrated solar power (CSP) technology is an important way to achieve sustainable development. Moving Packed Bed Heat Exchanger (MPBHE) has been key equipment in the waste energy recovery and CSP. Cheng et al. (2019) indicated that MPBHE is one of the promising candidates for recovering a large amount of waste heat from industrial solid bulk materials. In CSP, particles coupled with the supercritical CO_2 Brayton cycle is a potential way to improve the power generation efficiency compared with the molten salt (Ehsan et al., 2020). MPBHE becomes a cost-competitive alternative with less heat loss in CSP, compared with the fluidized bed.
The form of MPBHE includes the shell-and-tube (Baumann and Zunft, 2015) and the shell-and-plate (Albrecht and Ho, 2019). Particle flow is a gravity-driven flow in MPBHE. Compared with the shell-and-plate, the shell-and-tube has advantages in higher pressure bearing capacity and lower pressure drop of fluid. Improving particle/tube heat transfer is the key issue for the shell-and-tube moving packed bed heat exchanger. When particles flow around the tubes, the stagnation zone and the cavity zone form at the upstream and downstream regions of the tube. Takeuchi (1996) found that the stagnation zone of the tube was affected by the pitch of tubes rather than particles velocity. Al-Ansary et al. (2012) found that increasing the sand flow rate can significantly increase the heat transfer coefficient, and the vibration has a negative effect on the heat transfer. Guo et al. (2020) explored the influence of tube vibration by numerical simulation. The vibration of the tube can reduce the stagnation zone and the cavity zone at the bottom of the tube and cause the separation of particles from the tube side. Jiang et al. (2020) added the stirrer between aligned tubes, the stirrer promotes the particle migration and strengthens the heat transfer. Tian et al. (2021) proposed a new type of tube for the shell-and-tube moving packed bed heat exchanger. This new type of tube significantly improves heat transfer at the top and bottom of the tube. Guo et al. (2022) experimentally investigated the heat transfer of granular flow around the aligned tubes. The result shows that the flow rate has a significant effect on the mean heat transfer coefficients, and the flow structures are not strictly periodic. Herein, the effect of tube arrangement on the particle side is numerically studied by the discrete element method. The flow and heat transfer characteristics of particles

Paper Received: 14 April 2022; Revised: 12 May 2022; Accepted: 15 May 2022
Please cite this article as: Tian X., Jia H., Zhang J., Guo Z., Yang J., Wang Q., 2022, Numerical Study on Shell- and-Tube Moving Packed Bed Heat Exchanger: Effect of Tube Arrangement on the Particle Side, Chemical Engineering Transactions, 94, 187-192 DOI:10.3303/CET2294031

flowing around the staggered and aligned tubes are analysed.

2. Method and simulation

In this paper, the discrete element method (DEM) coupled with the heat transfer model is used to simulate the flow and heat transfer of particles flowing in a tube bank. DEM shows more beneficial to study the behavior of particles in the moving packed bed (Bartsch and Zunft, 2019), which detects the movement and interaction of all particles at each time step. The Hertz-Mindlin soft sphere model (Deng et al., 2020) was used to calculate the flow of particles by EDEM 2.6. For the heat transfer, heat conduction and heat radiation are considered. Heat convection is ignored due to the densely packed with low flow velocity in MPBHE. The conduction includes conduction inside particle, particle contact conduction and conduction through gas. The thermal resistance model is adopted to calculate the heat transfer. More detailed descriptions of the heat transfer model and validation can be found in previous work by Tian et al. (2021).

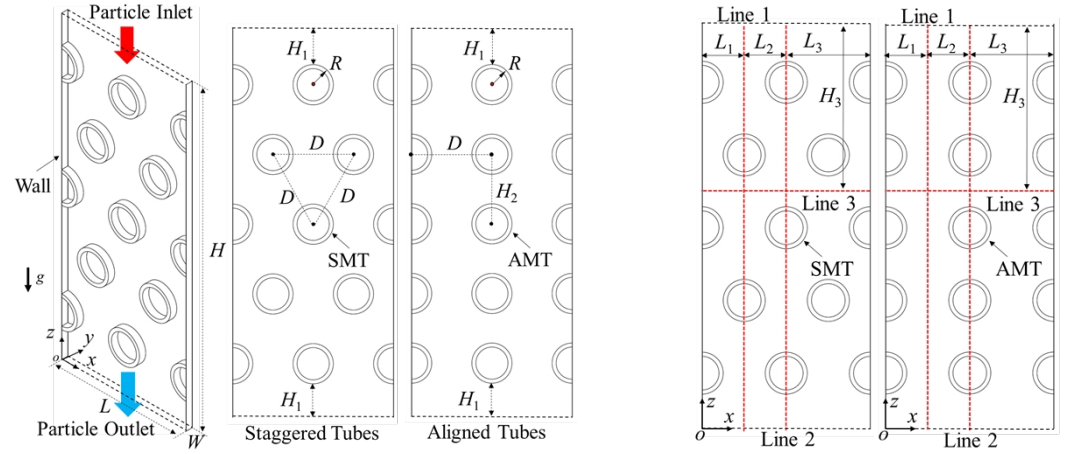

Figure 1: (a) Geometry model and (b) Schematic diagram of line1, line2 and line3

Table 1: Main parameters in the simulation

name	parameter	value	parameter	value	name	parameter	value
geometry	L (m)	0.12	H_1 (m)	0.026	particle	ρ (kg/m^3)	2,848
	W (m)	0.01	H_2 (m)	0.052		C_p (J/kg/K)	1,210
	H (m)	0.29	H_3 (m)	0.019		k_p (W/m/K)	0.55
	D (m)	0.06	L_1 (m)	0.03		E (Pa)	5.5×10^8
	R (m)	0.015	L_2 (m)	0.03		T_p (K)	700
	T_{tube} (K)	300	L_3 (m)	0.06		r_p (mm)	0.75

(L, W and H is the particle flow channel length, width and height; R is the tube radius; ρ is particle density; C_p is particle specific heat; k_p is particle thermal conductivity; E is Young's modulus; r_p is the particle radius.)

The geometry model used in the simulation is shown in Figure 1(a). The geometric model is mainly composed of tubes and channel walls. The size of the particle flow channel is L (length) × W (width) × H (height). For the tube arrangement, the staggered tubes and aligned tubes are arranged in the channel respectively. The tube center distance of the staggered tubes is equal to D. For aligned tubes, the horizontal distance of the tube center is equal to D and the vertical distance of the tube center is equal to H_2. The distance between the channel inlet/outlet and the top/bottom tubes is H_1. The outer radius of the tube is R. The geometric and physical parameters are shown in Table 1. Before the simulation, the randomly packed and high-temperature particles (T_p =800 K) are generated in the channel. The particle radius (r_p) is 0.75 mm. The initial velocity of the particles is equal to zero, and the particles fill the whole particle flow space of the tubes bank. During the simulation process, the tubes are kept at a constant temperature of 300 K and particles are constantly generated at the channel inlet to ensure that the packing height of particles in the channel is constant. The channel wall is adiabatic, and periodic boundary conditions are applied in the y direction. Particle velocity at the channel outlet, where the flow is controlled, remains constant in the vertical direction. Particle outlet velocity (v_{outlet}) is 5 mm/s. The simulated time step is equal to 2.3×10^{-6} s. The flow and heat transfer of particles are counted at each time

step during the simulation. The overall simulation lasts 60 s.

3. Results and discussion

In this section, the flow and heat transfer characteristics of particles flowing around the staggered and aligned tubes are analysed. The velocity distribution of particles flowing around the staggered tubes and aligned tubes at *t*=60 s is shown in Figure 2 (a). When particles flow around the staggered tubes, the stagnation zone and the cavity zone form at the upstream and downstream regions of the tube. The size and shape of the stagnation and cavity zones are different in different tube banks. There is no cavity zone at the downstream regions of the tube, when particles flow around the aligned tubes (except for the last row of tubes). The area between adjacent tubes in the vertical direction of the aligned tubes has the significant stagnation zone, and particles are locked in this zone by particles flowing in vertical channels between tubes. The stagnation zone above the aligned tubes is obviously larger than that of the staggered tubes.

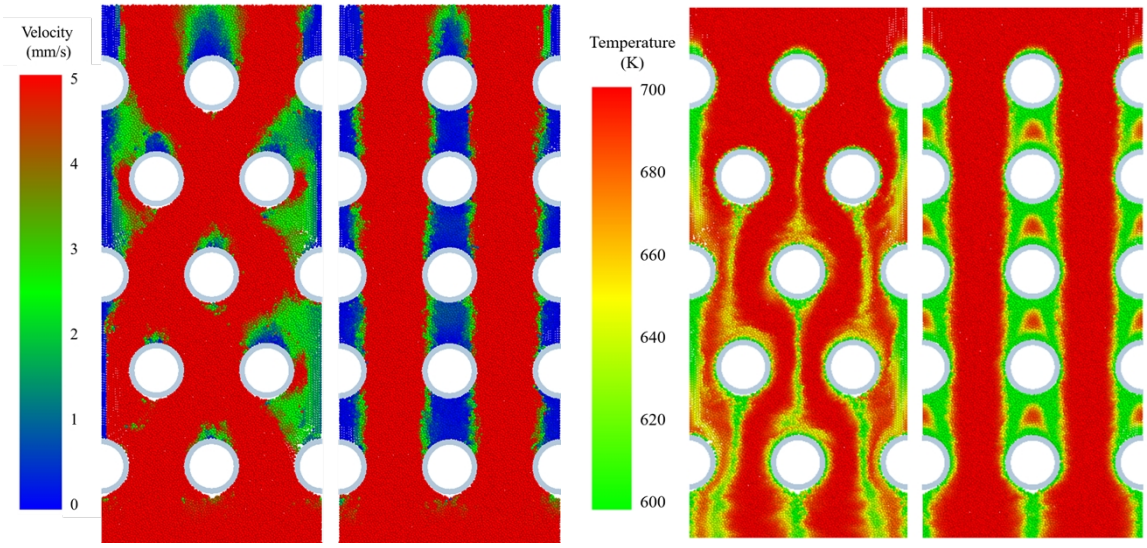

(a): Velocity distribution *(b): Temperature distribution*

Figure 2: Velocity and temperature distributions of particles flowing around the staggered tubes and aligned tubes at t=60 s

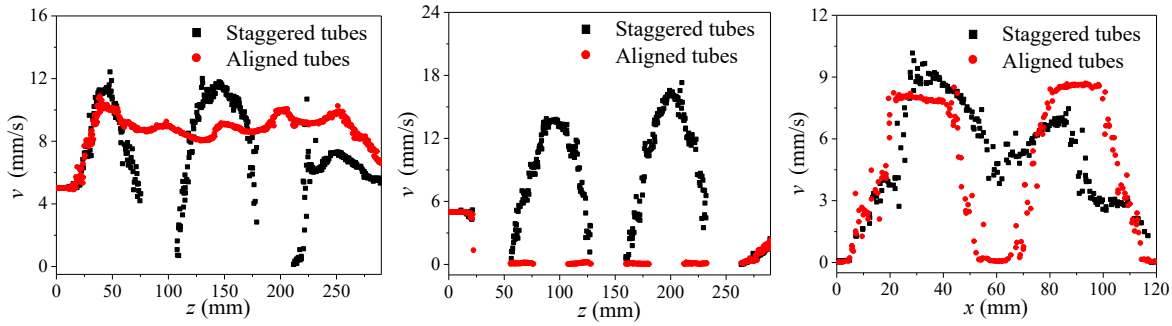

(a): Line 1 *(b): Line 2* *(c): Line 3*

Figure 3: Velocity distributions of different lines at t=60 s: (a)Line 1, (b) Line 2 and (c) Line 3

The velocity distributions of line 1, line 2 and line 3 obtained from Figure 2 (a) are shown in Figure 3. The information of these three lines can be found in Figure 1(b) and Table 1. In line1, the velocity of particles flowing around the aligned tubes is significantly higher than the outlet velocity. While the velocity of particles flowing around the aligned tubes is almost equal to zero in line2 of the stagnation zone, as shown in Figure 3(b). There is significant velocity gradient between particles in vertical channels and the stagnation zone, as shown in Figure 3(c). The particle velocity is the largest at the center of the adjacent tube in the horizontal direction, as shown in Figure 3. The temperature distribution of particles flowing around the staggered tubes and aligned tubes at

t=60 s is shown in Figure 2 (b). The temperature distributions of line 1, line 2 and line 3 obtained from Figure 2 (b) are shown in Figure 4. When particles flow around the aligned tubes, the particle temperature in the center of the vertical channels between tubes remains constant along the flow direction, as shown in Figure 2(b), Figure 4(a) and Figure 4(c). For the staggered tubes, the non-uniformity of velocity distribution leads to the non-uniformity of temperature distribution, especially in the top region of the tube. The particles temperature at the top and bottom of the tube in the staggered tubes is significantly higher than that in the aligned tubes, as shown in Figure 4(b). The temperature distribution of particles in different stagnation zone of the aligned tubes is almost the same, as shown in Figure 4(b) and Figure 4(c). The heat transfer rate (Φ) of the staggered tubes and aligned tubes with time is calculated as shown in Figure 5(a). At the beginning (t < 15 s), the heat transfer rate (Φ) of the staggered tubes is lower than that of the aligned tubes, because the top and bottom of the tube can contact with high-temperature particles in the aligned tubes. With the increase of time, the heat transfer rate (Φ) of the staggered tubes is higher than that of the aligned tubes. The heat transfer rate (Φ) of the staggered tubes increases by 21% compared with that of the aligned tubes at t= 60 s.

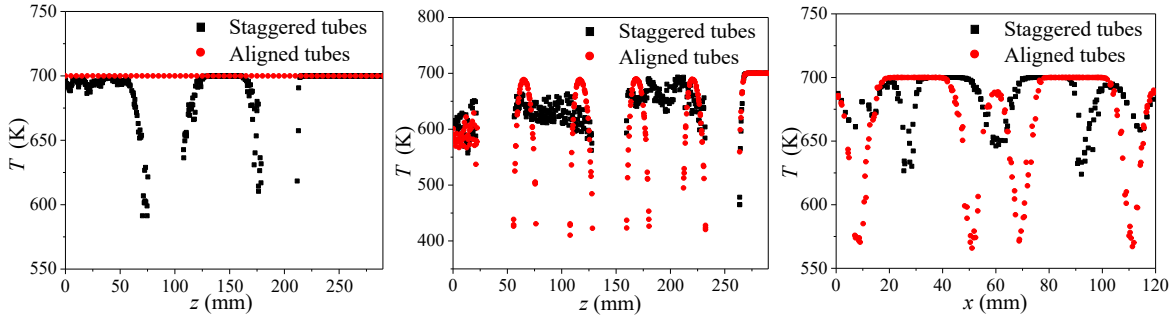

(a): Line 1 *(b): Line 2* *(c): Line 3*

Figure 4: Temperature distributions of different lines at t=60 s: (a)Line 1, (b) Line 2 and (c) Line 3

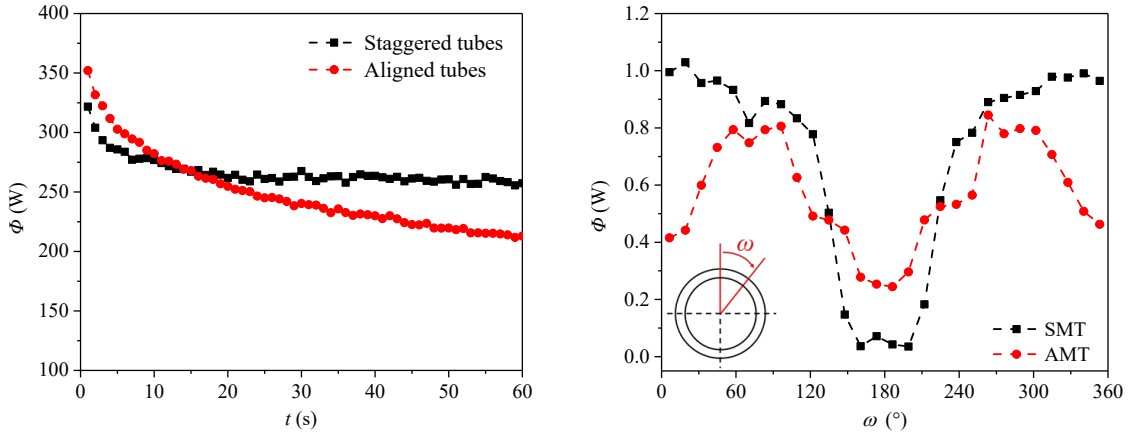

(a) *(b)*

Figure 5: (a) Variations of the heat transfer rate (Φ) of the staggered tubes and aligned tubes with time and (b) Variations of the heat transfer rate (Φ) of SMT and AMT with the angle at t=60 s

The flow and heat transfer characteristics of the middle tube of the tube bank will be analyzed in the following part. The middle tube of the staggered tubes (SMT) and the middle tube of the aligned tubes (AMT) are shown in Figure 1. The variations of the heat transfer rate (Φ) of SMT and AMT with the angle at t=60 s are shown in Figure 5(b). The velocity vector distributions of particles flowing around the SMT and the AMT at t=60 s are shown in Figure 6. The flow direction of particles varies with the surface of the SMT. A triangular stagnation zone is formed at the top of the SMT, and the cavity zone can be found at the bottom of the SMT, as shown in Figure 6(a). The flow direction of particles is almost along the direction of gravity on the tube side of the AMT. The obviously rectangular stagnation zones are formed at the top and bottom of the AMT, and the flow direction of particles is disordered, as shown in Figure 6(b). The heat transfer rate (Φ) at the side of the AMT (approximately between 60°-100° on both sides of the tube) is the highest as shown in Figure 5(b). The lowest

heat transfer rate (Φ) of the AMT is at the bottom of the tube, which is caused by the stagnation zone and bad contact. The heat transfer rate (Φ) of the SMT decreases gradually along the tube wall. The heat transfer rate (Φ) of the SMT decreased significantly in the range of 120°-160°, as shown in Figure 5(b). The lowest heat transfer rate (Φ) of the SMT is also at the bottom of the tube (approximately between 160°-200°), which is caused by the cavity zone.

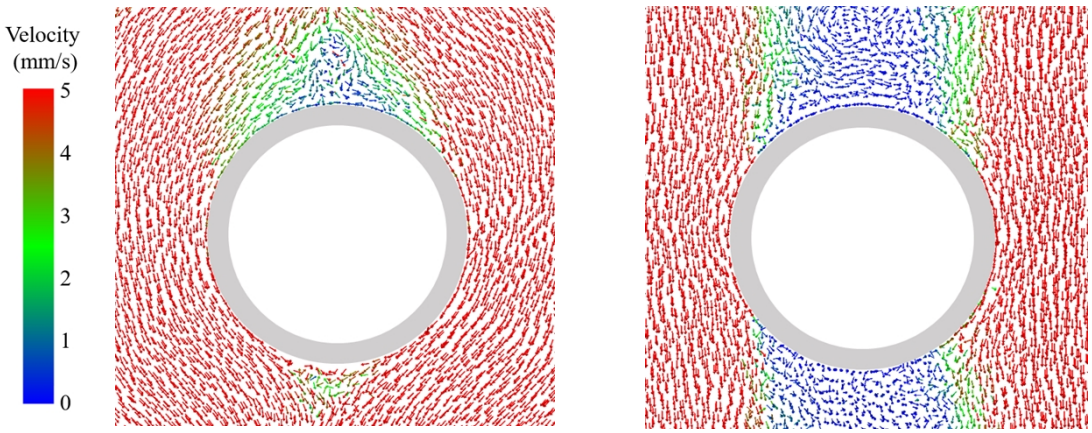

(a): SMT *(b): AMT*

Figure 6: Velocity vector distributions of particles flowing around the SMT and the AMT at t=60 s

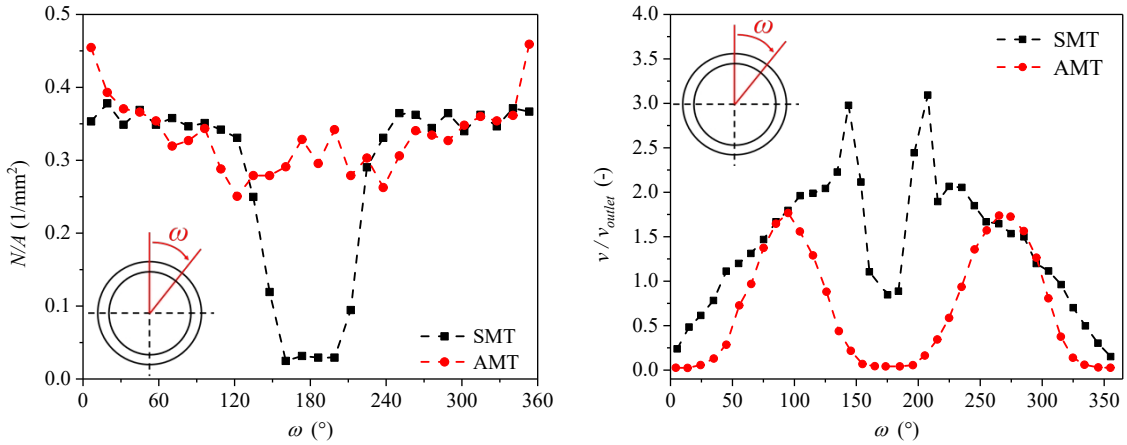

(a): Particle contact number distribution *(b): Dimensionless velocity distribution*

Figure 7: Particle contact number and dimensionless velocity distributions of particles flowing around the SMT and the AMT

The particle contact number and the time-averaged velocity are calculated along the angle of the tube. The velocity of particles in contact with the tube wall is used to calculate the time-averaged velocity. The particle contact number along the angle of the tube is shown in Figure 7(a). The particle contact number in Figure 7(a) is mostly symmetrical in the line chart. Variation within the half range of 0° < ω < 180° is analysed. The particle contact number of the SMT decreased significantly in the range of 120° - 160°, and the particle contact number of the SMT is almost equal to zero in the range of 160° - 180°, as shown in Figure 7(a). The highest particle contact number of the AMT is at the top of the tube, which is higher than that of the SMT. The lowest particle contact number of the AMT is at the ω = 120°, which may be due to the flow separation between particles and the tube wall as shown in Figure 6(b). The dimensionless velocity is obtained by the ratio of the time-averaged velocity to the outlet velocity, as shown in Figure 7(b). Variation within the half range of 0° < ω < 180° is analysed. The particle velocity increases with ω in the range of 0° - 145°, when particles flow around the SMT. When ω < 45°, the velocity of particle of the SMT is lower than the outlet velocity, and the stagnation zone is formed in this range. The particle velocity of the SMT decreased significantly in the range of 145° - 180°. The highest particle velocity of the AMT is at ω = 95°, as shown in Figure 7(b). The particle velocity of the AMT is less than the outlet velocity in the range of 0° - 65° and 125° - 180°, and the stagnation zone is defined in this range. The particle

velocity of the AMT increases first and then decreases in the range of 30°-150°.

4. Conclusions

In the present study, the effect of tube arrangement on the particle side for the shell-and-tube moving packed bed heat exchanger was investigated by the discrete element method. The flow and heat transfer characteristics of particles flowing around the staggered and aligned tubes are analysed. The major findings are summarized as below:

(i) The tube arrangement has a significant effect on the flow and heat transfer on the particle side. The triangular stagnation zone and the cavity zone are formed around the staggered tubes. The rectangular stagnation zones are formed at the top and bottom of the tube in the aligned tubes, which means there is no cavity zone at the bottom of the tube.

(ii) The heat transfer performance of the staggered tubes is better than that of the aligned tubes. The heat transfer at the side tube of the aligned tubes and the top tube of the staggered tubes are the best. The bottom of the tube has the worst heat transfer in both the staggered and aligned tubes.

(iii) The stagnation zone of the staggered tubes is in the range of 0° - 45°, and the cavity zone of the staggered tubes is in the range of 160° - 180°. The stagnation zone of the aligned tubes is in the range of 0°- 65° and 125° - 180°. The highest particle velocity in the aligned tubes appears at 95°.

The current research shows that the staggered tubes are a better configuration for the MPBHE. However, more factors need to be considered such as tube spacing, particle diameter, velocity, etc. For the staggered tubes, it is necessary to optimize the flow and heat transfer in the range 0° - 45° and 160° - 180°. For the aligned tubes, reducing the vertical tube spacing to fill the stagnation zone may be an effective option to enhance heat transfer.

Acknowledgements

The work is financially supported by National Natural Science Foundation of China (No. 52076169).

References

Al-Ansary H., El-Leathy A., Al-Suhaibani Z., Jeter S., Sadowski D., Alrished A., Golob M., 2012, Experimental study of a sand-air heat exchanger for use with a high-temperature solar gas turbine system, Journal of Solar Energy Engineering - Transactions of the ASME, 134, 041017.

Albrecht K.J., Ho C.K., 2019, Design and operating considerations for a shell-and-plate, moving packed bed, particle-to-sCO_2 heat exchanger, Solar Energy,178, 331–340.

Bartsch P., Zunft S., 2019, Granular flow around the horizontal tubes of a particle heat exchanger: DEM-simulation and experimental validation, Solar Energy, 182, 48–56.

Baumann T., Zunft S., 2015, Development and performance assessment of a moving bed heat exchanger for solar central receiver power plants, Energy Procedia, 69, 748-757.

Cheng Z.L., Guo Z.G., Tan Z.T., Yang J., Wang Q.W., 2019, Waste heat recovery from high temperature solid granular materials: Energy challenges and opportunities, Renewable and Sustainable Energy Reviews, 116,109428.

Deng S., Wen Z., Lou G., Zhang D., Su F., Liu X., Dou R., 2020, Process of particles flow across staggered tubes in moving bed, Chemical Engineering Science, 217, 115507.

Ehsan M.M., Guan Z., Gurgenci H., Klimenko A., 2020, Feasibility of dry cooling in supercritical CO_2 power cycle in concentrated solar power application: Review and a case study, Renewable and Sustainable Energy Reviews, 132, 110055.

Guo Z.G., Zhang S., Tian X., Yang J., Wang Q.W., 2020, Numerical investigation of tube oscillation in gravity-driven granular flow with heat transfer by discrete element method, Energy, 207, 118203.

Guo Z.G., Tian X., Wu Z.H., Yang J., Wang Q.W., 2022, Heat transfer of granular flow around aligned tube bank in moving bed: Experimental study and theoretical prediction by thermal resistance model, Energy Conversion and Management, 257, 115435.

Jiang B.F., Xia D.H., Zhang H.L., Pei H., Liu X.J., 2020, Effective waste heat recovery from industrial high-temperature granules: A Moving Bed Indirect Heat Exchanger with embedded agitation, Energy, 208, 118346.

Takeuchi H., 1996, Particles Flow Pattern and Local Heat Transfer Around Tube in Moving Bed, AIChE Journal, 42, 1621–1626.

Tian X., Guo Z.G., Jia H.N., Yang J., Wang Q.W., 2021, Numerical investigation of a new type tube for shell-and-tube moving packed bed heat exchanger, Powder Technology, 394, 584–596.